SPANDIDOS PUBLICATIONS

MOLECULAR MEDICINE REPORTS 27: 30, 2023

S100A1 expression is increased in spinal cord injury and promotes inflammation, oxidative stress and apoptosis of PC12 cells induced by LPS via ERK signaling

YE BAI[1,2], NING GUO[3], ZHANWU XU[2], YUXI CHEN[1], WENJIN ZHANG[2], QINGHE CHEN[2] and ZHENGGANG BI[1]

[1]Department of Orthopedics, The First Affiliated Hospital of Harbin Medical University; Departments of [2]Orthopaedics and [3]Outpatient, The 962nd Hospital of The People's Liberation Army Joint Logistic Support Force, Harbin, Heilongjiang 150000, P.R. China

Received August 21, 2022; Accepted November 24, 2022

DOI: 10.3892/mmr.2022.12917

Abstract. Spinal cord injury (SCI) is a severe neurological disorder and the molecular mechanisms leading to its poor prognosis remain to be elucidated. S100A1, a mediator of Ca^{2+} handling of sarcoplasmic reticulum and mitochondrial function, operates as an endogenous danger signal (alarmin) associated with inflammatory response and tissue injury. The aim of the present study was to investigate the expression and biological effects of S100A1 in SCI. A rat model of SCI and a PC12 cell model of lipopolysaccharide (LPS)-induced inflammation were established to examine S100A1 expression at the mRNA and protein levels. The inflammation level, which was mediated by S100A1, was determined based on inflammatory factor (IL-1β, IL-6 and TNF-α) and anti-inflammatory factor (IL-10) expression. The effects of S100A1 on cellular oxidation and anti-oxidation levels were observed by detecting the levels of reactive oxygen species, superoxide dismutase, catalase activities and nuclear factor erythroid 2-related factor 2 expression. The protein levels of Bax, Bcl2 and cleaved caspase-3 were used for the evaluation of the effects of S100A1 on apoptosis. Phosphorylated (p-)ERK1/2 expression was used to evaluate the effects of S100A1 on ERK signaling. The results revealed that S100A1 expression was significantly upregulated *in vivo* and *in vitro* in the PC12 cell model of LPS-inflammation. The silencing and overexpression of S100A1 helped alleviate and aggravate LPS-induced inflammation, oxidative stress and apoptosis levels, respectively. S100A1 was found to regulate the ERK signaling pathway positively. An inhibitor of ERK signaling (MK-8353) partially abolished the promoting effects of the overexpression of S100A1 on inflammation, oxidative stress damage and apoptosis. In conclusion, S100A1 expression was elevated in model of SCI and in the PC12 cell model of LPS-induced inflammation. Furthermore, the overexpression/silencing S100A1 aggravated/mitigated the inflammation, oxidative stress damage and the apoptosis of LPS-stimulated PC12 cells via the ERK signaling pathway. The present study revealed the mechanism of S100A1 in SCI, which provided a new theoretic reference for future research on SCI.

Correspondence to: Dr Zhenggang Bi, Department of Orthopedics, The First Affiliated Hospital of Harbin Medical University, Harbin, Heilongjiang 150000, P.R. China
E-mail: bizhenggang2020@163.com

Key words: spinal cord injury, S100A1, ERK, inflammation, oxidative stress damage, apoptosis

Introduction

Spinal cord injury (SCI) is known as a fatal neurological disorder characterized by motor, sensory, or autonomic function deficits and has led to a heavy economic burden on patients and society (1,2). As reported in 2016, there was a total of 282,000 individuals suffering from SCI in the United States and the rate of annual occurrence was found to be 54 cases per million individuals (~17,000 new cases per year) (3). Although great progress has been made in the development of strategies for neuroprotection and neuroregeneration with the development of drugs (1), surgery (4), stem cell transplantation (5) and tissue engineering technology (6), these strategies have not achieved satisfactory therapeutic efficacy clinically (7). This suggests that the understanding of the mechanisms of SCI progression remain to be elucidated.

The main pathogenesis of SCI is the inflammation dominated by activated microglia and astrocytes in the injured site after the primary mechanical injury (8). It has been reported that the levels of inflammatory factors, including TNF-α, IL-1β and IL-6 are elevated following SCI (9). Furthermore, the excessive production of pro-inflammatory cytokines can promote the generation of reactive oxygen species (ROS), leading to oxidative damage (10). On the other hand, the loss of blood supply to the injured site directly leads to an increase in ROS generation (11). This microenvironment composed of various inflammatory mediators leads directly to the apoptosis of functional cells, such as neurons (12). Therefore, a comprehensive understanding of the inflammatory mechanisms following SCI is necessary in order to providing a more theoretical basis for the treatment of SCI in the future.

S100A1, belonging to the S100 protein family, has been reported to regulate the release, uptake and transport of calcium by regulating calcium ATPase, leading to the activity of cellular signals (13). An imbalance in S100A1 has been revealed to induce the further impairment of myocardial viability and function on hypoxia-induced cell dysfunction in cardiovascular disease (13-15). Furthermore, S100A1 can bind to Toll-like receptor 4 (TRL4), which in turn activates the nuclear factor κB (NF-κB) and mitogen-activated protein kinases (MAPK) pathways, well-known drivers of inflammation, in cardiovascular and respiratory diseases (15,16), suggesting that S100A1 is a crucial inflammatory mediator, particularly under the conditions of ischemia and hypoxia. At the same time, S100A1 plays a critical role in the nervous system. A previous study demonstrated that S100A1 aggravated neuroinflammation and disease histopathology in a mouse model of Alzheimer's disease (17). In addition, the ablation of S100A1 in PC12 cells has been found to maintain cell viability and increase resistance to amyloid-β peptide-induced cell apoptosis (18). Extracellular signal-regulated kinase (ERK), downstream of NF-κB, has been reported to be a critical target of the apoptosis of nerve cells. Blocking the activity of ERK can attenuate neuroinflammation and neuroapoptosis (19). However, whether S100A1 can affect the function of neuronal cells through ERK activity remains to be fully determined.

In the present study, S100A1 expression was detected in a rat SCI model *in vivo* and a PC12 cell model *in vitro* of lipopolysaccharide (LPS)-induced inflammation. Next, it was determined whether ERK signaling activity was a downstream target of S100A1 by observing whether ERK signaling activity changed with S100A1 expression. Finally, whether S100A1 could affect the inflammation, oxidative stress and apoptosis of PC12 induced by LPS through ERK signaling pathway was explored. The present study revealed the expression and mechanism of S100A1 in SCI, providing a new reference for the study of SCI.

Materials and methods

Establishment of rat model of SCI. A total of 10 male Sprague-Dawley rats (age, 11-12 weeks; weight, 200-230 g) were obtained from the Experimental Animal Center of Harbin Medical University and were divided into the sham-operated (Sham; n=5) and SCI group (n=5). All rats were raised in the isolated ventilation cage at 22-26˚C, 50% relative humidity with a 12/12-h light/dark cycle and had free access to sterile water and granular food. The rats in the sham group were only subjected to dorsal laminectomy of the T10 vertebral body, while the rats in the SCI group were subjected to spinal cord contusion surgery at the level of T10 as previously described (20). All rats were observed for health and behavior status once a day for seven consecutive days after surgery and were administered with penicillin (1 ml; 160,000 U/ml) and meloxicam (4 mg/kg) in the first three days to prevent infection and relieve pain. Uncontrollable inflammatory response at the wound site was set as the humane endpoints in the study (21). The study was reviewed and approved by the Ethics Committee of The First Affiliated Hospital of Harbin Medical University (Harbin, China; approval no. 2021080) and all experiments were carried out in accordance with the guidelines of Animal Care and Use Committee of the Harbin Medical University.

Euthanasia of experimental animals and sample handling. The animal experiment lasted for 7 days. On the 7th day after the surgery, all 10 rats had survived without infection/death and were anesthetized by an intraperitoneal injection of 1% sodium pentobarbital (40 mg/kg, MilliporeSigma). Death was confirmed by observing lack of heartbeat, breathing and pupils and nerve reflexes of the rats for 5 min (22). Then, 1 ml blood was collected through the orbital venous plexus for ELISA. Subsequently, the rats were euthanized via excessive anesthesia (3% sodium pentobarbital; 160 mg/kg), as previously described (23). After the whole body was perfused with cool saline, the site of injury was removed together with 5 mm of upper and lower spinal cord tissue. The samples used for western blot analysis and reverse transcription-quantitative PCR (RT-qPCR) were stored in liquid nitrogen, while the samples used for histochemistry were stored in 4% paraformaldehyde.

PC12 cell culture and treatment. LPS can induce inflammation in PC12 cells via TLR4 activity and it is widely used for SCI model *in vitro* (24-26). In the present study, the PC12 cells induced by LPS was used for the SCI model *in vitro*. PC12 cells, harvested from the pheochromocytoma of the rat adrenal medulla, no adrenaline secretion and comprised of eosinophilic and neuroblastic cells (27), were obtained from the Cell Resource Center of the Chinese Academy of Sciences (Shanghai Institute of Biological Sciences) and cultured in RPMI-1640 medium (HyClone; Cytiva) containing 10% fetal bovine serum (Gibco; Thermo Fisher Scientific, Inc.) in 5% CO_2 and a 37˚C humidified atmosphere. The culture medium was changed every 2-3 days and the cells were sub-cultured when the cell density reached 90%. LPS, extracted from *Escherichia coli* 055:B5, at 1, 5 and 10 μg/ml (cat. no. L8880; Beijing Solarbio Science & Technology Co., Ltd.), configured one night in advance and stored overnight, was used to establish a PC12 cell model of inflammation for subsequent research.

RT-qPCR. The mRNA expression levels of S100A1, IL-1β, IL-6, IL-10 and TNF-α were evaluated using RT-qPCR. Total RNA from the spinal cord tissue and PC12 cells was isolated using TRIzol® reagent (Invitrogen; Thermo Fisher Scientific, Inc.) according to the manufacturer's instructions. A total of 1 μg RNA was used for cDNA reverse transcription with the reverse transcription kit (Takara Bio, Inc.) following the manufacturer's instructions. Lastly, the TB Green® Premix Ex Taq II kit (Takara Bio, Inc.) was used for qPCR with the following thermocycling conditions: Pre-heating at 95˚C for 10 min, followed by 45 cycles at 95˚C for 15 sec, at 60˚C for 30 sec and at 72˚C for 30 sec as previously described (22). The primer sequences used in the present study are listed in Table I. GAPDH was used as the internal reference. The relative expression levels of target genes were calculated using the $2^{-\Delta\Delta Cq}$ formula (28).

Western blot analysis. Briefly, total protein from the spinal cord tissue and PC12 cells was isolated using RIPA buffer

Table I. Primers sequences used in reverse transcription-quantitative PCR.

Gene	Forward primer (5'-3')	Reverse primer (5'-3')
S100A1	ggtcggcagtaaagacaggt	atttcagcagcacacggttg
IL-1β	gcacagttccccaactggta	ggagactgcccattctcgac
IL-6	acaagtccggagaggagact	acagtgcatcatcgctgttc
TNF-α	atgggctccctctcatcagt	gcttggtggtttgctacgac
IL-10	ttccctgggagagaagctga	gacacctttgtcttggagctta
CAT	gctccgcaatcctacaccat	ggacatcgggtttctgaggg
MnSOD	caccgaggagaagtaccacg	tgggttctccaccacccctta
GAPDH	gcatcttcttgtgcagtgcc	ggtaaccaggcgtccgatac

(Beyotime Institute of Biotechnology) containing 1 mM PMSF (Dalian Meilun Biology Technology Co., Ltd.) on the ice for 30 min. After the protein concentration was detected using a BCA kit (Beyotime Institute of Biotechnology), 60-80 μg protein was loaded on 12.5 or 15% SDS-PAGE for separation, followed by transfer onto a PVDF membrane (Merck KGaA). The membrane was first blocked with 5% skimmed milk in 0.05% PBS-Tween 20 for 1 h at room temperature. The membranes were then incubated with primary antibodies for S100A1 (1:500; cat. no. 16027-1-AP; ProteinTech Group, Inc.), nuclear factor erythroid 2-related factor 2 (Nrf2; 1:1,000; cat. no. 80593-1-RR; ProteinTech Group, Inc.), ERK1/2 (1:1,000; cat. no. 4695), p-ERK1/2 (1:2,000; cat. no. 4370), cleaved caspase-3 (1:1,000; cat. no. 9664), Bax (1:1,000; cat. no. 2772), Bcl2 (1:1,000; cat. no. 3498) (all from Cell Signaling Technology, Inc.) and β-actin (1:1,000; cat. no. 20536-1-AP; ProteinTech Group, Inc.) overnight at 4°C followed by incubation with HRP-conjugated secondary antibody (1:10,000; cat. no. 7074, Cell Signaling Technology, Inc.) at room temperature for 1 h. Lastly, the bands were visualized using ECL reagent (Beyotime Institute of Biotechnology) as per the manufacturer's protocol with the ChemiDoc MP System (Bio-Rad Laboratories, Inc.). The semi-quantitative analysis was performed with Image-Pro Plus (version 6.0; Media Cybernetics, Inc.).

Cell transfection. S100A1 overexpression (ov-S100A1) plasmid (plasmid primer: Forward: 5'-GAAGATTCTAGAGCTAGC GAATTCATGGGCTCTGAGCTGGAG-3'; Reverse: 5'-CGC AGATCCTTGCGGCCGCGGATCCTCAACTGTTCTCCC AGAA-3') encoding the full-length open reading frame of rat S100A1 and the S100A1 short-interfering (si) RNA plasmid targeting sequence (5'-UGGAGACCCUCAUCAAUGUdT dT-3') for silencing S1001A (si-S100A1), as well as their corresponding blank plasmid vectors were prepared by Shanghai Genechem Co., Ltd. The overexpression and silencing of S100A1 in PC12 cells were carried out using Lipofectamine® 3000 (Invitrogen; Thermo Fisher Scientific, Inc.) according to the manufacturer's instructions. At 48 h post-transfection, the PC12 cells with gene intervention were exposed to LPS and were used in other experiments. In addition, the cells transfected with ov-S100A1 plasmid were treated with the ERK inhibitor, MK-8353 (100 nM, MedChemExpress), 12 h prior to exposure to LPS, as previously described (29). The cell groups were designed as follows: The control group (without any treatment), LPS group (cells stimulated with 5 μg/ml LPS), LPS + si-S100A1, LPS + ov-S100A1 and ov-S100A1 with MK-8353 treatment (LPS + ov-S100A1 + MK) groups.

Hematoxylin and eosin (HE) staining. The HE staining was performed to compare the histomorphological differences between the SCI and Sham groups. Briefly, the spinal cord tissues were fixed with 4% paraformaldehyde at 4°C for 24 h and prepared as paraffin-embedded tissues after dehydration using xylene and gradient alcohol solution. Next, 5-μm paraffin sections were prepared, heated in the 60°C oven for 30 min and washed with xylene I and II, for 5 min each time at room temperature. After being treating with 100, 100, 95, 95 and 80% gradient alcohol at room temperature for 5 min each time, the sections were stained using the HE stain kit (Beijing Solarbio Science & Technology Co., Ltd.) according to the manufacturer's instructions. Firstly, the sections were treated with hematoxylin for 1 min at room temperature, followed by being differentiated in 1% hydrochloric acid for 30 sec at room temperature. Lastly, the sections were stained with eosin for 2 min at room temperature. Finally, the images were harvested by light microscope (Leica Microsystems GmbH).

Tissue immunofluorescence. Immunofluorescence assay was performed to explore the changes in S100A1 expression in SCI *in vivo*. The spinal cord tissues were fixed with 4% paraformaldehyde at 4°C for 24 h, then dehydrated by sucrose solution gradient and embedded in optimal cutting temperature compound to yield 5-μm-thick frozen sections. Following incubation with 0.3% H_2O_2 at room temperature for 30 min, 0.5% Triton X-100 was used for permeabilizing the sections. Normal goat serum (10%; Beijing Zhongshan Jinqiao Biotechnology Co., Ltd.) was then used to incubate the sections at room temperature for 30 min. After the primary antibody of S100A1 (1:50; cat. no. 16027-1-AP; ProteinTech Group, Inc.) was used to incubate the sections overnight at 4°C, the fluorescent secondary antibody (1:500; cat. no. ab150113, Abcam) was used to incubate the sections for 1 h at room temperature. Lastly, the cell nuclei were stained with DAPI (Beijing Solarbio Science & Technology Co., Ltd.) for 5 min at room temperature and the sections were visualized using a fluorescence microscope (Olympus Corporation). Image-Pro Plus (version 6.0; Media Cybernetics, Inc.) was used for statistical analysis.

Cell immunofluorescence. In order to detect the changes in the expression of S100A1 in PC12 cells stimulated with various concentrations of LPS, a density of $2x10^5$ cells/well was seeded in six-well plates and cultured overnight followed by stimulation with 1, 5 and 10 μg/ml LPS for 12 h at 37°C. The cells were then fixed with 4% paraformaldehyde for 30 min at room temperature and permeabilized with 0.5% Triton X-100 for 30 min at room temperature. Subsequently, the cells were blocked with 5% BSA for 30 min (Beijing Solarbio Science & Technology Co., Ltd.) at room temperature and incubated with S100A1 primary antibody (1:100; cat. no. 16027-1-AP; ProteinTech Group, Inc.) overnight at 4°C. The fluorescent secondary antibody (1:500; cat. no. ab150113, Abcam) and

DAPI were used to treat the cells for 1 h and 5 min at room temperature, respectively. Images were obtained using a fluorescence microscope (Olympus Corporation). Image-Pro Plus (version 6.0; Media Cybernetics, Inc.) was used for analysis.

ELISA. ELISA was performed to examine the effects of S100A1 on inflammation levels in the PC12 cell culture supernatant. The cell supernatant among different groups was collected and the expression levels of IL-1β (cat. no. KE20005; ProteinTech Group, Inc.), IL-6 (cat. no. KET9004-96T; EliKine; Abbkine Scientific Co., Ltd.), TNF-α (cat. no. KE20001; ProteinTech Group, Inc.) and IL-10 (cat. no. KE20003; ProteinTech Group, Inc.) were detected using the respective kits according to the manufacturer's instructions.

ROS level evaluation. The levels ROS among different groups were evaluated using the 2'-7'-dichlorodihydrofluorescein-diacetate (DCFH-DA) kit (Beyotime Institute of Biotechnology) according to the manufacturer's instructions. Briefly, the cells from the different groups were collected following trypsin digestion and incubated with serum-free medium (Gibco; Thermo Fisher Scientific, Inc.) containing DCFH-DA (10 μM) probes for 30 min in the dark at room temperature. The cells were then resuspended by PBS following centrifugation (201 x g) at room temperature for 5 min. The DCFH-DA-positive cells were detected using a flow cytometer (BD FACSCalibur; BD Biosciences).

Activity detection of catalase (CAT) and manganese superoxide dismutase (MnSOD). The activities of CAT and MnSOD among different groups were evaluated using CAT and MnSOD Assay kits (Nanjing Jiancheng Bioengineering Institute) based on the cell lysate. Briefly, the cells from the different groups were harvested followed by resuspension with 0.3 ml PBS. Next, after the resuspended cells being broken by ultrasound (frequency, once every 2 sec) on ice for 1 min (Scientz-IID), the protein was harvested with centrifugation (13,887 x g for 25 min at 4˚C). The total protein concentration was detected using a BCA kit (Beyotime Institute of Biotechnology). The contents of CAT and MnSOD in the samples were examined according to the corresponding manufacturer's instructions.

Apoptosis assay. The cellular apoptosis levels of the control, si-S100A1, ov-S100A1 and ov-S100A1 + MK groups were evaluated using an apoptosis kit (cat. no. CA1020 Beijing Solarbio Science & Technology Co., Ltd.) according to the manufacturer's instructions. First, the cells from the different groups were collected following trypsin digestion and incubated with solution containing propidium iodide and Annexin V for 10 min in the dark at room temperature. The sample was then resuspended in PBS following centrifugation (201 x g) at room temperature for 5 min and detected using a flow cytometer (BD FACSCalibur; BD Biosciences).

Statistical analysis. All experiments in the present study were conducted at least three times. The data were analyzed using GraphPad Prism 6.0 software (GraphPad Software, Inc.) and are presented as the mean ± standard deviation. An unpaired t-test was used for comparisons between two groups. For comparisons between multiple groups, when n<6, Kruskal Wallis test of multiple independent samples were performed. P<0.05 was considered to indicate a statistically significant difference.

Results

S100A1 expression is elevated in tissue from rats with SCI. With the aim of exploring the expression of S100A1 in SCI, a rat model of SCI was first established. Subsequently, the morphological examination revealed that there were evident tissue defects, hemorrhaging, necrosis and inflammatory cell infiltration, as well as nerve cell atrophy and vacuolization in the SCI group compared with the Sham group (Fig. 1A); this suggested that the model of SCI was successfully established. The mRNA and protein expression levels of S100A1 were found to be significantly upregulated in the SCI group compared with the Sham group (Fig. 1B and C). Furthermore, immunofluorescence staining confirmed that S100A1 was highly expressed in the tissue of rats with SCI, compared with that of the rats in the Sham group (Fig. 1D). Finally, the aforementioned results confirmed that S100A1 was significantly upregulated in the tissue of rats with SCI.

S100A1 expression is upregulated in the PC12 cell model of LPS-induced inflammation. PC12 cells are widely used in neural dysfunction-related research, including SCI (30). In the present study, S100A1 expression was detected in the PC12 cell model of LPS-induced inflammation. After the PC12 cells were stimulated with various concentrations of LPS (0, 1, 5 and 10 μg/ml) for 12 h, the mRNA and protein expression levels of S100A1 exhibited a significant increase in a concentration-dependent manner (Fig. 2A and B). The results of immunofluorescence staining also revealed that the expression of S100A1 was elevated with the increasing LPS concentration (Fig. 2C). On the whole, these results suggested that S100A1 expression was upregulated in the PC12 cell model of LPS-induced inflammation. Subsequently, 5 μg/ml LPS was used for PC12 cell model establishment to explore the biological function of S00A1 in LPS induced SCI model *in vitro* as the reported studies (30-32).

S100A1 expression mediates the activity of the ERK signaling pathway in PC12 cells stimulated with LPS. S100A1 expression was upregulated in the rats with SCI and in cells with stimulated with LPS *in vitro*. However, the potential function of S100A1 in PC12 cells stimulated with LPS remained unclear. Plasmids containing siRNA targeting S100A1 and the full length of S100A1 were used to silence and overexpress S100A1, respectively and the results were verified using western blot analysis. S100A1 expression was significantly decreased in the si-S100A1 group and significantly increased in the ov-S100A1 group, compared with the control group (Fig. 3A). The ERK signaling pathway has been verified to be associated with the inflammation process and blocking its activity can effectively attenuate inflammatory injury induced by oxygen-glucose deprivation and the reperfusion of PC12 cells (33-35). Similarly, in the present study, the silencing or overexpression of S100A1 was accompanied by the partially decreased or increased expression of p-ERK1/2, respectively,

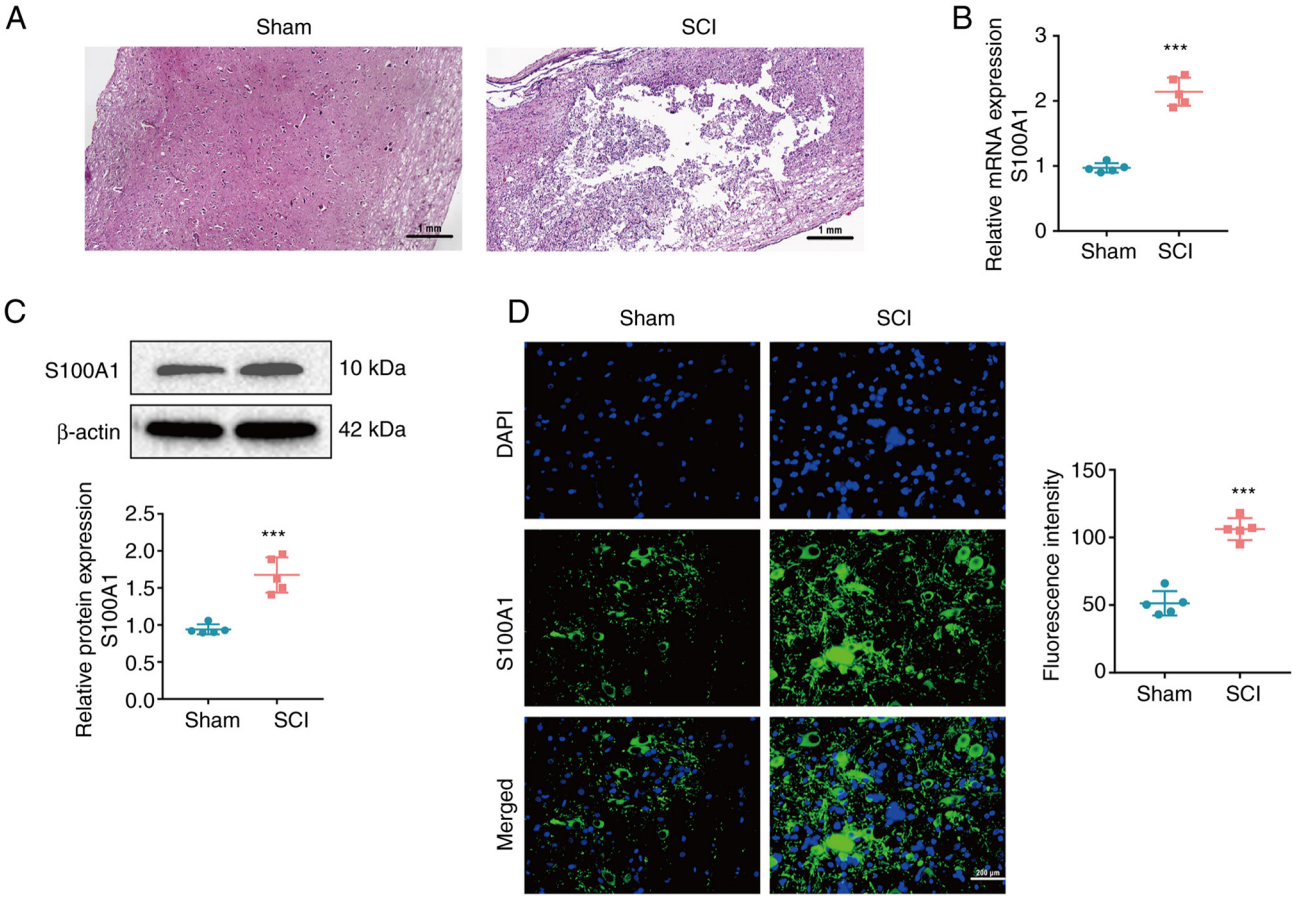

Figure 1. S100A1 expression in SCI. (A) Representative images of hematoxylin and eosin staining in the Sham and SCI group on the sagittal plane (scale bar, 1 mm). (B) mRNA expression of S100A1 in the Sham and SCI group examined using reverse transcription-quantitative PCR. (C) The protein expression of S100A1 in the Sham and SCI group was examined using western blot analysis. (D) The expression of S100A1 in the Sham and SCI group was verified using immunofluorescence staining (scale bar, 200 μm). n=5. ***P<0.001 vs. Sham group. SCI, spinal cord injury; Sham, sham-operated.

indicating that changes in S100A1 expression could mediate the activity of the ERK signaling pathway in PC12 cells (Fig. 3B).

S100A1 regulates the inflammation of PC12 cells by mediating the ERK signaling pathway. As SCI is accompanied by the inflammatory cascade, effective strategies for suppressing inflammatory injury may contribute to functional recovery following SCI (8). Whether S100A1 could regulate the inflammation level of PC12 cells *in vitro* was explored. First, the mRNA and protein secretion levels of pro-inflammatory cytokines (IL-1β, IL-6 and TNF-α), as well as anti-inflammatory cytokines (IL-10) were detected. As was expected, following stimulation with LPS, the expression levels of IL-1β, IL-6 and TNF-α in the LPS group were significantly higher in comparison with the control group, while the expression of IL-10 exhibited the opposite trend (Fig. 4A and B). However, the silencing of S100A1 partially attenuated the levels of inflammatory mediators in the cells and improved their anti-inflammatory ability (Fig. 4A and B). The overexpression of S100A1 aggravated the levels of inflammation and these effects were partially abolished by the ERK1/2 molecular inhibitor, MK-8353 (Fig. 4A and B). These results suggested that S100A1 could mediate the levels of inflammation of PC12 cells by targeting the ERK signaling pathway.

S100A1 regulates the oxidative-stress damage of PC12 cells by mediating the ERK signaling pathway. Oxidative stress-induced damage is highly associated with inflammation and tissue ischemia and necrosis caused by SCI are the common causes of oxidative stress-induced injury (36). In the present study, as expected, the levels of ROS were found to be significantly elevated in the LPS group (Fig. 5A and B). At the same time, the silencing of S100A1 partially decreased the level of ROS and the overexpression of S100A1 promoted the generation of ROS. Similarly, the ERK1/2 inhibitor, MK-8353, partially prevented the promoting effects of the overexpression of S100A1 on ROS generation (Fig. 5A and B). Furthermore, the effects of S100A1 on the antioxidant capacity of cells were evaluated. The enzymatic activities, CAT and MnSOD, decreased significantly in the LPS group. The silencing expression of S100A1 promoted the gene expression and enzyme activity of CAT and MnSOD, while the overexpression of S100A1 further decreased the levels of CAT and MnSOD. In addition, MK-8353 partially counteracted the inhibitory effects of S100A1 overexpression on CAT and MnSOD levels (Fig. 5C and D). Nrf2, is a transcription factor of anti-oxidative stress element and its increased expression can transfer it to the nucleus and participate in the transcription of CAT and SOD, leading to the enhancement of cell antioxidant capacity (37). Herein, the protein expression of Nrf2 was detected among the

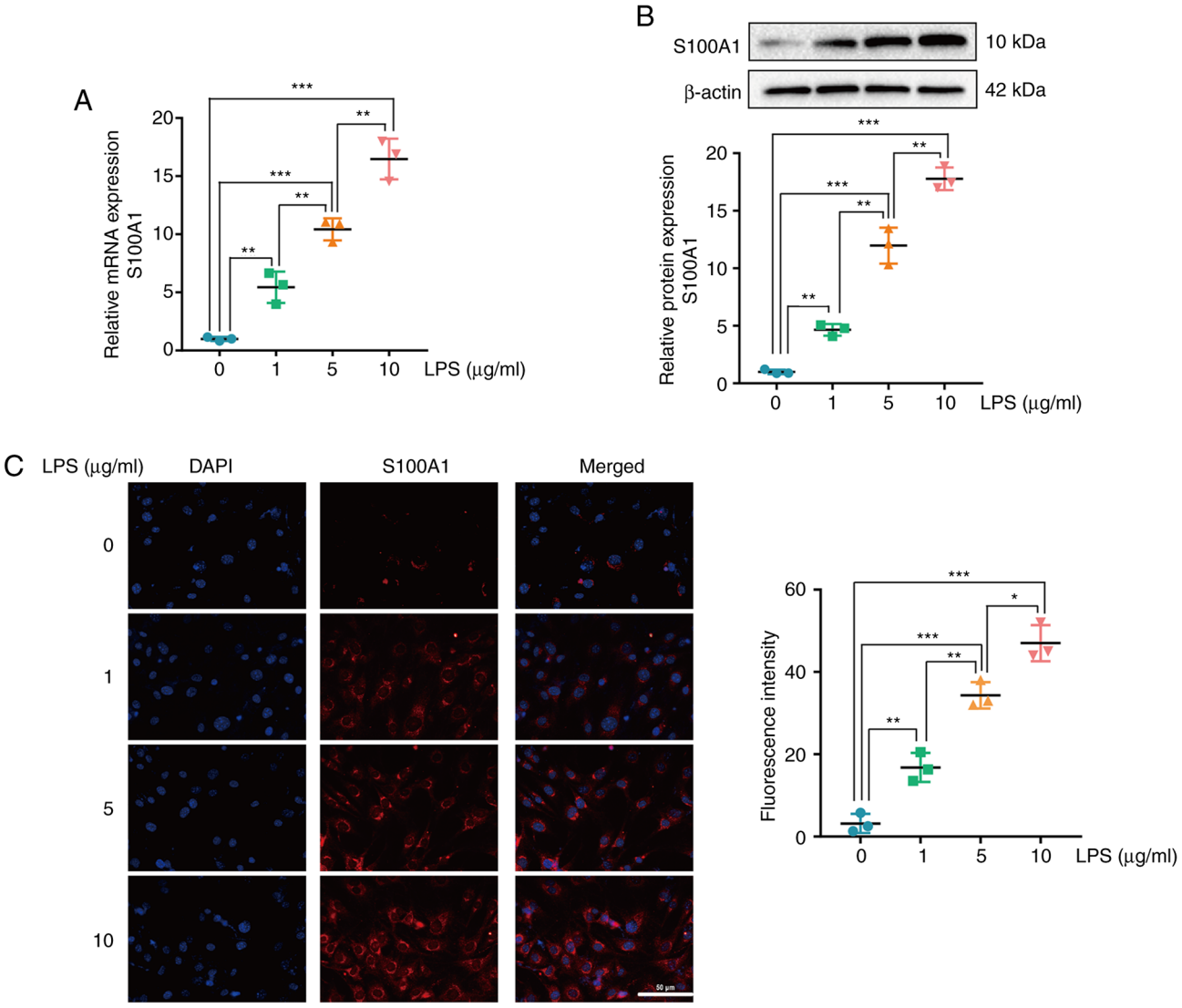

Figure 2. S100A1 expression in LPS-stimulated PC12 cells. (A) S100A1 mRNA expression was detected using reverse transcription-quantitative PCR in PC12 cells stimulated with various concentrations of LPS. (B) S100A1 protein expression was detected using western blot analysis in PC12 cells stimulated with various concentrations of LPS. (C) S100A1 protein expression was examined using immunofluorescence staining in PC12 cells stimulated with various concentrations of LPS (scale bar, 50 μm). n=3. *P<0.05, **P<0.01, ***P<0.001. LPS, lipopolysaccharide.

groups and found that Nrf2 expression decreased significantly in the LPS group. Silencing and overexpression of S100A1 accompanied by up- and down-regulated Nrf2 expression. MK-8353 partially counteracted the inhibitory effects of S100A1 overexpression on Nrf2 level (Fig. 5E) Thus, these results suggested that S100A1 regulated the oxidative stress levels in PC12 cells by targeting the ERK signaling pathway.

S100A1 regulates the apoptosis of PC12 cells by mediating the ERK signaling pathway. Retaining a sufficient number of viable cells is the crucial factor limiting the progression of SCI (38). Thus, the present study investigated the effects of S100A1 on the level of apoptosis. It was found that the level of apoptosis was elevated by LPS stimulation. The silencing and overexpression of S100A1 significantly decreased and increased apoptosis level, respectively. In addition, MK-8353 partly abolished the promoting effects of S100A1 overexpression on apoptosis (Fig. 6A and B). Subsequently, the effects of S100A1 on apoptosis related proteins were also detected. The ratio of Bax/Bcl2 was increased in the LPS group, whereas it was partially decreased in the LPS + si-S100A1 group and further increased in the LPS + ov-S100A1 group (Fig. 6C). In addition, the expression of cleaved caspase-3 also exhibited a similar trend of Bax/Bcl2 (Fig. 6D). As was expected, MK-8353 partially abolished the promoting effect of S100A1 overexpression on the expression of Bax/Bcl2 and cleaved caspase-3 (Fig. 6C and D). These results suggested that S100A1 regulated the apoptosis of PC12 cells by targeting the ERK signaling pathway.

Discussion

With the development of modern medical technology, SCI remains a significant source of mortality and is associated with increasing costs for society, as a result of long-term disability. Although there some preclinical studies on stem cells (39), gene therapy (40) or tissue engineering technology (41) for neuroprotection and regeneration have been performed, few

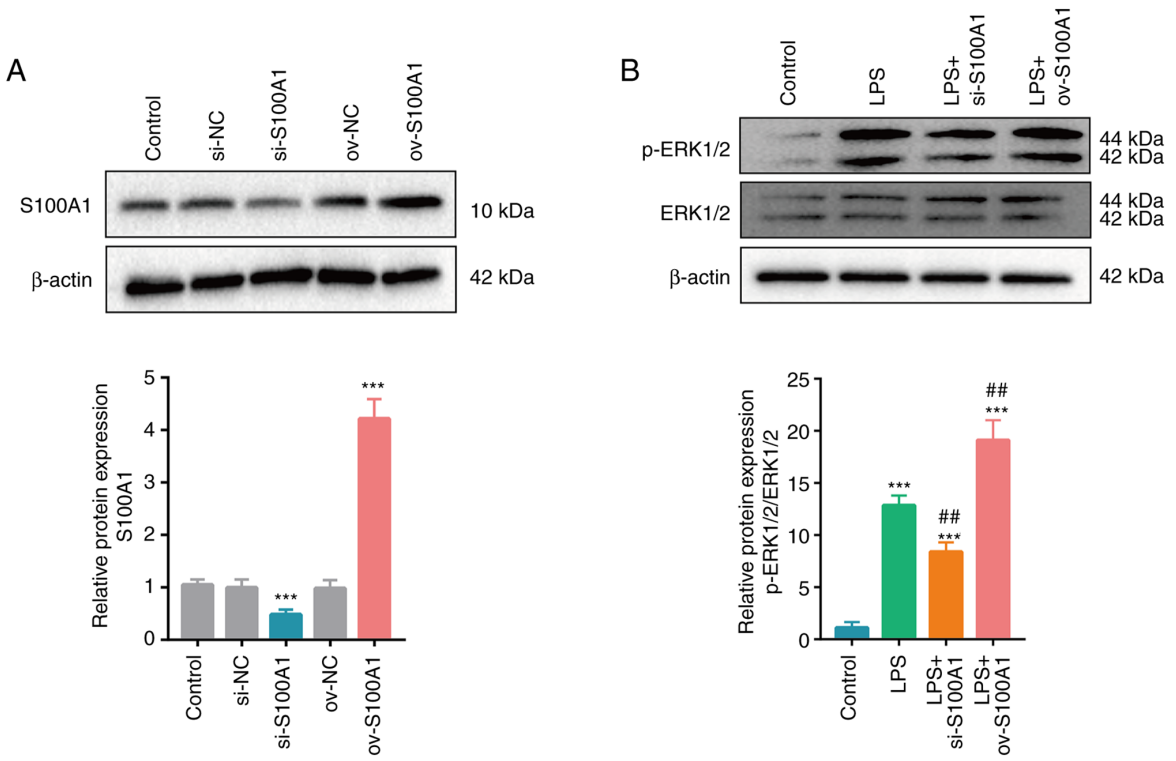

Figure 3. S100A1 positively regulates the ERK signaling pathway. (A) S100A1 protein expression after the silencing and overexpression of S100A1 in PC12 cells was detected using western blot analysis. (B) Expression of p-ERK1/2 and total ERK1/2 expression in the Control, LPS, LPS with silencing and S100A1 overexpression groups. n=3. ***P<0.001 vs. Control group. $^{\#\#}$P<0.01 vs. LPS group. LPS, lipopolysaccharide; si, short interfering; ov, overexpression; NC, negative control; p-, phosphorylated.

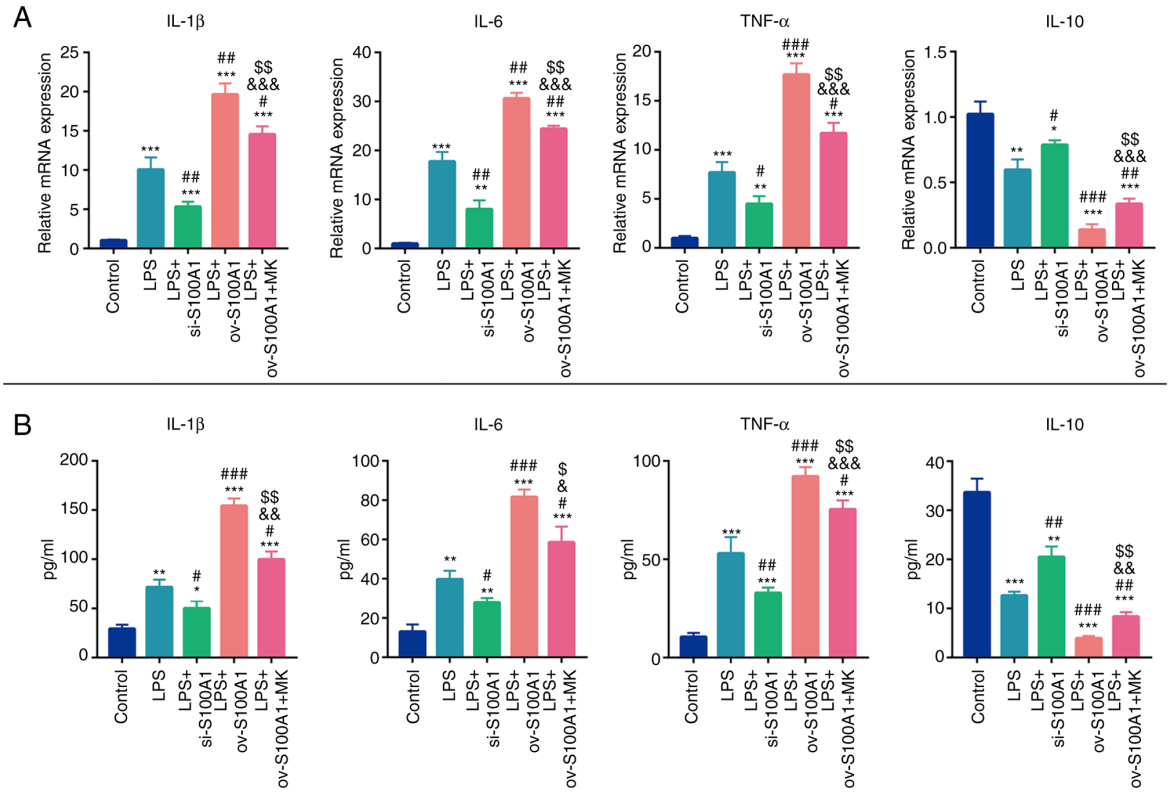

Figure 4. S100A1 regulates the level of inflammation in PC12 cells through the ERK signaling pathway. (A) The mRNA expression levels of inflammatory cytokines (IL-1β, IL-6 and TNF-α) and anti-inflammatory cytokines (IL-10) were detected using reverse transcription-quantitative PCR in the Control, LPS, LPS with S100A1 silencing/overexpression, LPS with S100A1 overexpression and EKR inhibitor groups. (B) The protein levels of inflammatory cytokines (IL-1β, IL-6 and TNF-α) and anti-inflammatory cytokines (IL-10) were detected using ELISA in the Control, LPS, LPS with S100A1 silencing/overexpression, LPS with S100A1 overexpression and EKR inhibitor groups. n=3. *P<0.05, **P<0.01, ***P<0.001 vs. Control group. $^{\#}$P<0.05, $^{\#\#}$P<0.01, $^{\#\#\#}$P<0.001 vs. LPS group. $^{\&}$P<0.05, $^{\&\&}$P<0.01 vs. LPS + si-S100A1 group. $^{\$}$P<0.05, $^{\$\$}$P<0.01 vs. LPS + ov-S100A1 group. LPS, lipopolysaccharide; ov, overexpression; si, short interfering.

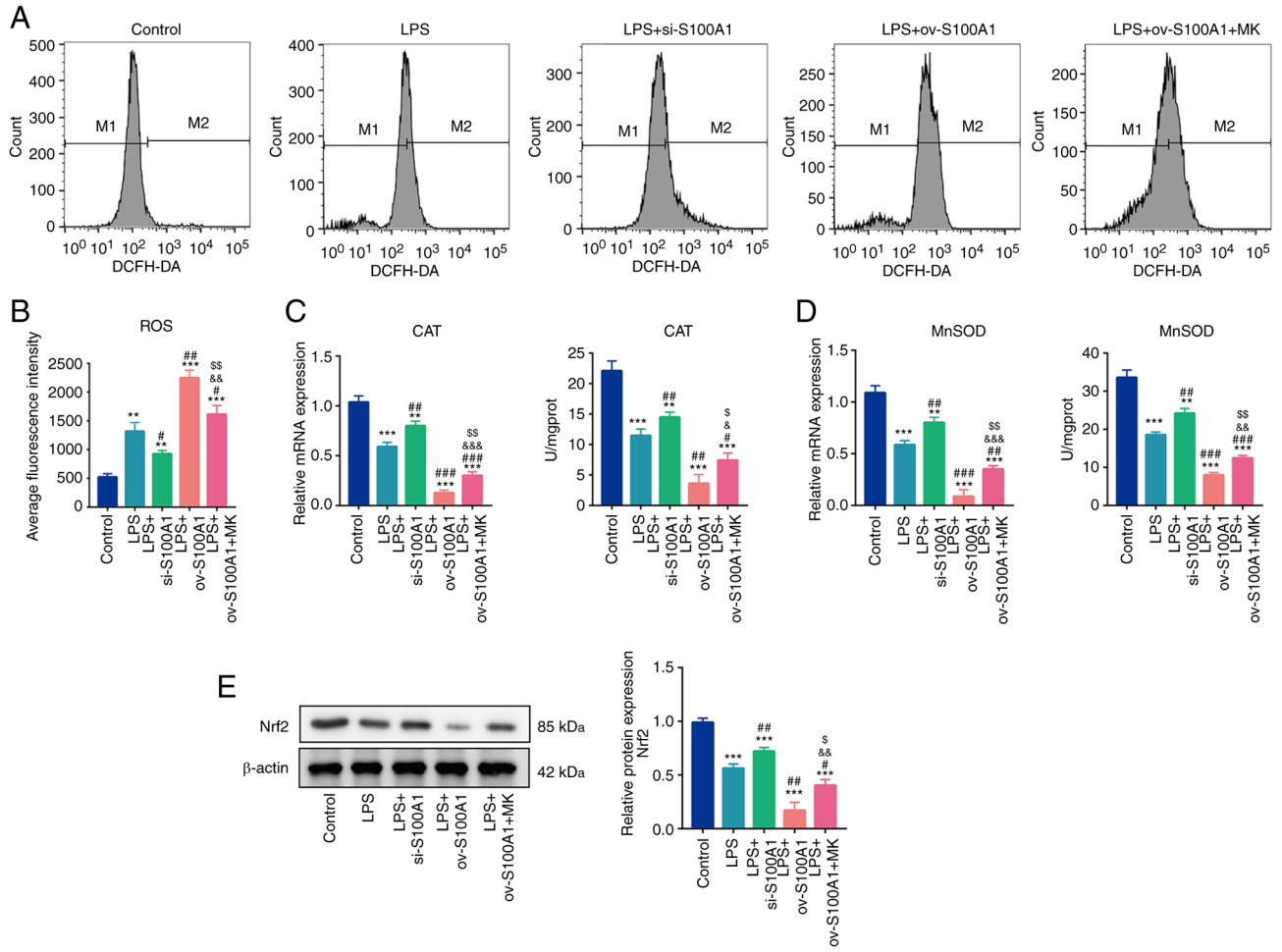

Figure 5. S100A1 regulates the oxidative stress levels of PC12 cells through the ERK signaling pathway. (A and B) ROS levels in the Control, LPS, LPS + S100A1 silencing/overexpression, LPS with S100A1 overexpression and EKR inhibitor groups. (C) mRNA and enzyme activity of CAT in the different groups. (D) mRNA and enzyme activity of MnSOD in the different groups. (E) The protein expression of Nrf2 in differnet groups, n=3. **P<0.01, ***P<0.001 vs. Control group. $^{\#}$P<0.05, $^{\#\#}$P<0.01, $^{\#\#\#}$P<0.001 vs. LPS group. $^{\&}$P<0.05, $^{\&\&}$P<0.01, $^{\&\&\&}$P<0.001 vs. LPS + si-S100A1. $^{\$}$P<0.05, $^{\$\$}$P<0.01 vs. LPS + ov-S100A1 group. LPS, lipopolysaccharide; ROS, reactive oxygen species; CAT, catalase; MnSOD, manganese superoxide dismutase; ov, overexpression; si, short interfering; Nrf2, nuclear factor erythroid 2-related factor 2.

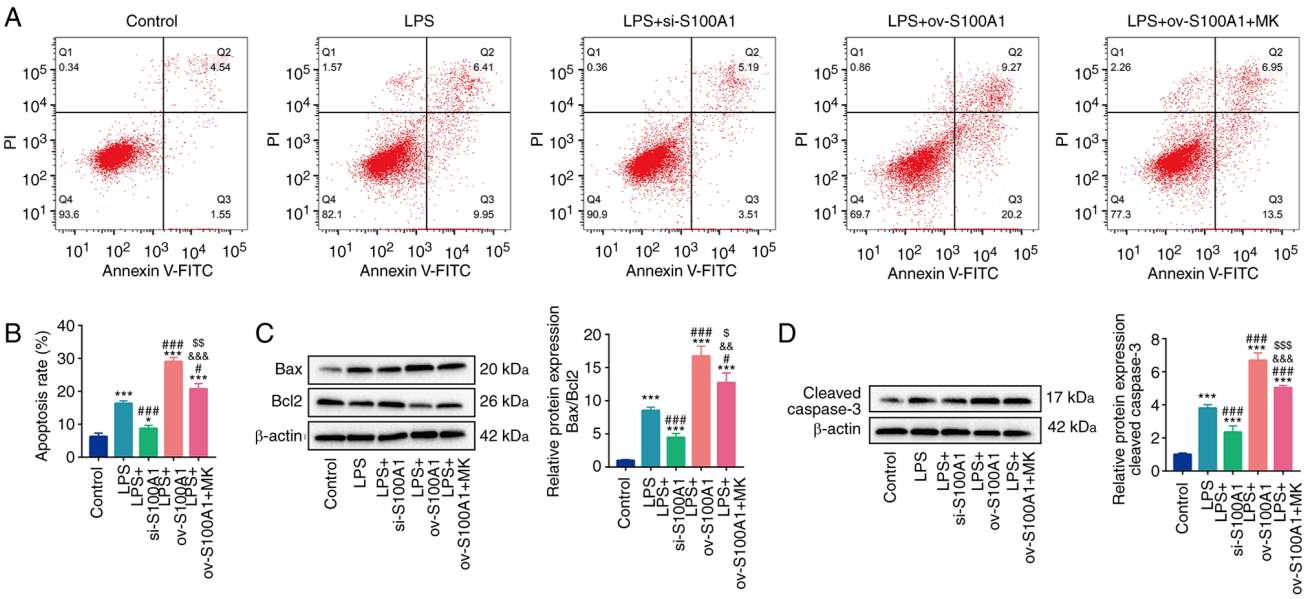

Figure 6. S100A1 regulates the apoptosis of PC12 cells through the ERK signaling pathway. (A and B) The apoptosis levels in the Control, LPS, LPS with S100A1 silencing/overexpression, LPS with S100A1 overexpression and EKR inhibitor groups. (C and D) The protein levels of Bax, Bcl2 and cleaved caspase-3 in the different groups. n=3. *P<0.05, ***P<0.001 vs. Control group. $^{\#}$P<0.05, $^{\#\#\#}$P<0.001 vs. LPS group. $^{\&\&}$P<0.01, $^{\&\&\&}$P<0.001 vs. LPS + si-S100A1. $^{\$}$P<0.05, $^{\$\$}$P<0.01, $^{\$\$\$}$P<0.001 vs. LPS + ov-S100A1 group. LPS, lipopolysaccharide; ov, overexpression; si, short interfering.

investigations have reached clinic practice (35). Thus, a more in-depth understanding of the molecular basis of SCI is still required. In the present study, S100A1 was found to be significantly highly expressed in the damaged spinal cord tissue. In addition, S100A1 was also found to be highly expressed in the PC12 cell model of LPS induced-inflammation. Furthermore, silencing the expression of S100A1 partially inhibited inflammation, oxidative stress-induced damage and apoptosis via the ERK signaling pathway in PC12 cells stimulated with LPS.

The main pathological structures of SCI include primary injury followed by the secondary injury. The primary injury involves mechanical compression and damage caused by fractured and/or displaced bone fragments. Current clinical approaches towards primary injury mainly include early surgical decompression and stabilization (42). The spinal cord tissue squeezed by external forces is followed by ischemia, hypoxia and the excessive release of inflammatory cytokines and prostaglandins, resulting in oxidative stress-induced injury and more severe tissue apoptosis and necrosis (43,44). Nevertheless, at present, there are no available effective treatments for the inflammatory process of SCI (42), even though a number of research teams have verified that anti-inflammatory treatment can exert an effective neuroprotective effect in animal experimental models (45-47). However, the majority of research results are still far from real clinical transformation. Thus, the investigation of the inflammatory pathological process of SCI is still necessary so as to develop practical and effective treatments.

S100A1 is a member of the S100 protein family and serves as an alarmin in injured tissue, such as the heart or/and cardiomyocytes (15). S100A1 is mainly involved in the regulation of sarcoplasmic reticulum Ca^{2+} activity, as well as mitochondrial function and participates in cellular activities (48). In a previous study, S100A1 was found to be released from the ischemic myocardium to the circulation of patients and mice with acute ST-segment (15). At the same time, S100A1 plays an early immunomodulatory role in cardiac fibroblasts of injured hearts (15). In addition, the inhibition of S100A1 expression has been shown to mitigate oxidative stress and the apoptosis of cardiomyocytes (49,50). However, the expression of S100A1 in the injured spinal cord and its regulatory effects on inflammation, oxidative stress and apoptosis remain to be elucidated.

In the present study, S100A1 was verified to be highly expressed *in vivo* and in PC12 cells stimulated with LPS *in vitro*, accompanied by increased levels of inflammation, oxidative stress-induced damage and apoptosis. The silencing of S100A1 partially reduced the LPS-induced inflammation, oxidative stress and apoptosis, whereas the overexpression of S100A1 aggravated inflammation, oxidative stress and the apoptosis of PC12 *in vitro*.

ERK1/2 signaling, as a crucial component of the MAPK pathway, is an evolutionary conserved signaling cascade, responsible for transmitting signals from the cell surface to inside the cells (33). Furthermore, it has been reported that ERK1/2 signaling can mediate the development process of the neuronal system and can participate in certain neurological activities by regulating nerve growth, elastic properties, neurological and cognitive processing in nerve injuries (51). In addition, the inhibition of ERK1/2 can block the cellular inflammatory and apoptosis response of PC12 (33). However, whether S100A1 can regulate the ERK signaling pathway in PC12 cells remains unclear.

In the present study, it was found that the stimulation of PC12 cells with LPS activated the ERK signaling pathway. The silencing of S100A1 partially reduced the activity of ERK and the overexpression of S100A1 promoted the activation of the ERK signaling pathway, suggesting that S100A1 can regulate the activity of ERK signaling as upstream signal. In addition, the ERK inhibitor, MK-8353 partly abolished the promoting effects of the overexpression of S100A1 on inflammation, oxidative stress and the apoptosis of PC12 cells. These results verified that S100A1 regulated the inflammation, oxidative stress and apoptosis of PC12 cells via the ERK signaling pathway.

It is worth noting that although MK-8353 application significantly reduced the levels of inflammation, oxidative stress and apoptosis compared with LPS + ov-S100A1 group, MK-8353 application did not decrease these phenotypes levels of cells like LPS + si-S100A1 group, suggesting the increase of S100A1 leaded to the increase of inflammation, oxidative stress and apoptosis of PC12 cells partly through ERK signaling pathway. As expected for the ERK signaling pathway in the present study, PI3K, Wnt/β-catenin, NF-κB signaling and others are all reported to be involved in SCI development (52-54). MK-8353 application blocked the activity of ERK but did not block other possible mechanisms that were potential regulated by SA100A1. This may be the reason why the application of MK-8353 can only partially reduce the inflammation, oxidative stress and apoptosis levels of cells. The typical downstream mechanisms of S100A1 will continue to be explored in subsequent studies.

There were still some limitations in the present study. First, LPS was used to induce PC12 cells to simulate SCI *in vitro*. LPS causes inflammatory reaction by activating TLR4 molecules in cells (55). Although TLR4 activation is also a mechanism of SCI (56), the LPS induced cell model does not fully represent the mechanism of SCI *in vivo*. In addition, the results of the present study have not been supplemented *in vivo*, which is another limitation of the study.

In conclusion, in the present study, S100A1 expression was upregulated in rats with SCI and in LPS-stimulated PC12 cells. The overexpression of S100A1 was accompanied by an increase in inflammation, oxidative stress injury and apoptosis. The silencing of S100A1 attenuated inflammation, oxidative stress and apoptosis by blocking the ERK signaling pathway. Thus, the present study revealed the expression and mechanisms of S100A1 in SCI. These findings may provide more references for the future theoretical research of SCI.

Acknowledgements

Not applicable.

Funding

No funding was received.

Availability of data and materials

The datasets used and/or analyzed during the current study are available from the corresponding author on reasonable request.

Authors' contributions

YB and ZB were substantially responsible for the experiment conception and design. YB, NG, ZX and YC contributed to data acquisition and statistical analysis. YB, WZ and QC were responsible for the interpretation of the experimental data, drafting the manuscript and revising it critically for important intellectual content. YB and ZB confirm the authenticity of all the raw data. All authors read and approved the final version of the manuscript.

Ethics approval and consent to participate

The present study obtained the approval of the ethics committee of The First Affiliated Hospital of Harbin Medical University (grant no. 2021080).

Patient consent for publication

Not applicable.

Competing interests

The authors declare that they have no competing interests.

References

1. Ahuja CS, Wilson JR, Nori S, Kotter MRN, Druschel C, Curt A and Fehlings MG: Traumatic spinal cord injury. Nat Rev Dis Primers 3: 17018, 2017.
2. Alizadeh A, Dyck SM and Karimi-Abdolrezaee S: Traumatic spinal cord injury: An overview of pathophysiology, models and acute injury mechanisms. Front Neurol 10: 282, 2019.
3. Spinal Cord Injury (SCI) 2016 facts and figures at a glance. J Spinal Cord Med 39: 493-494, 2016.
4. Ahuja CS, Nori S, Tetreault L, Wilson J, Kwon B, Harrop J, Choi D and Fehlings MG: Traumatic spinal cord injury-repair and regeneration. Neurosurgery 80 (Suppl 1): S9-S22, 2017.
5. Sabapathy V, Tharion G and Kumar S: Cell therapy augments functional recovery subsequent to spinal cord injury under experimental conditions. Stem Cells Int 2015: 132172, 2015.
6. Raspa A, Pugliese R, Maleki M and Gelain F: Recent therapeutic approaches for spinal cord injury. Biotechnol Bioeng 113: 253-259, 2016.
7. Fan B, Wei Z, Yao X, Shi G, Cheng X, Zhou X, Zhou H, Ning G, Kong X and Feng S: Microenvironment imbalance of spinal cord injury. Cell Transplant 27: 853-866, 2018.
8. Hutson TH and Di Giovanni S: The translational landscape in spinal cord injury: Focus on neuroplasticity and regeneration. Nat Rev Neurol 15: 732-745, 2019.
9. Bareyre FM and Schwab ME: Inflammation, degeneration and regeneration in the injured spinal cord: Insights from DNA microarrays. Trends Neurosci 26: 555-563, 2003.
10. Filippin LI, Vercelino R, Marroni NP and Xavier RM: Redox signalling and the inflammatory response in rheumatoid arthritis. Clin Exp Immunol 152: 415-422, 2008.
11. Hazzaa SM, Abdou AG, Ibraheim EO, Salem EA, Hassan MHA and Abdel-Razek HAD: Effect of L-carnitine and atorvastatin on a rat model of ischemia-reperfusion injury of spinal cord. J Immunoassay Immunochemistry 42: 596-619, 2021.
12. Donnelly DJ and Popovich PG: Inflammation and its role in neuroprotection, axonal regeneration and functional recovery after spinal cord injury. Exp Neurol 209: 378-388, 2008.
13. Yu J, Lu Y, Li Y, Xiao L, Xing Y, Li Y and Wu L: Role of S100A1 in hypoxia-induced inflammatory response in cardiomyocytes via TLR4/ROS/NF-κB pathway. J Pharm Pharmacol 67: 1240-1250, 2015.
14. Bashir M, Frigiola A, Iskander I, Said HM, Aboulgar H, Frulio R, Bruschettini P, Michetti F, Florio P, Pinzauti S, *et al*: Urinary S100A1B and S100BB to predict hypoxic ischemic encephalopathy at term. Front Biosci (Elite Ed) 1: 560-567, 2009.
15. Rohde D, Schön C, Boerries M, Didrihsone I, Ritterhoff J, Kubatzky KF, Völkers M, Herzog N, Mähler M, Tsoporis JN, *et al*: S100A1 is released from ischemic cardiomyocytes and signals myocardial damage via Toll-like receptor 4. EMBO Mol Med 6: 778-794, 2014.
16. Haw TJ, Starkey MR, Pavlidis S, Fricker M, Arthurs AL, Nair PM, Liu G, Hanish I, Kim RY, Foster PS, *et al*: Toll-like receptor 2 and 4 have opposing roles in the pathogenesis of cigarette smoke-induced chronic obstructive pulmonary disease. Am J Physiol Lung Cell Mol Physiol 314: L298-L317, 2018.
17. Afanador L, Roltsch EA, Holcomb L, Campbell KS, Keeling DA, Zhang Y and Zimmer DB: The Ca^{2+} sensor S100A1 modulates neuroinflammation, histopathology and Akt activity in the PSAPP Alzheimer's disease mouse model. Cell Calcium 56: 68-80, 2014.
18. Zimmer DB, Chaplin J, Baldwin A and Rast M: S100-mediated signal transduction in the nervous system and neurological diseases. Cell Mol Biol (Noisy-le-Grand) 51: 201-214, 2005.
19. Park JH, Seo YH, Jang JH, Jeong CH, Lee S and Park B: Asiatic acid attenuates methamphetamine-induced neuroinflammation and neurotoxicity through blocking of NF-kB/STAT3/ERK and mitochondria-mediated apoptosis pathway. J Neuroinflammation 14: 240, 2017.
20. Jing Y, Yu Y, Bai F, Wang L, Yang D, Zhang C, Qin C, Yang M, Zhang D, Zhu Y, *et al*: Effect of fecal microbiota transplantation on neurological restoration in a spinal cord injury mouse model: Involvement of brain-gut axis. Microbiome 9: 59, 2021.
21. Howard B, Nevalainen T and Perretta G: The COST manual of laboratory animal care and use: Refinement, Reduction, and Research. Crc Press, 2010.
22. Sun F, Zhang H, Huang T, Shi J, Wei T and Wang Y: S100A9 blockade improves the functional recovery after spinal cord injury via mediating neutrophil infiltration. Ex Ther Med 23: 291, 2022.
23. Li Y, Liu P and Wei F: Long non-coding RNA MBI-52 inhibits the development of liver fibrosis by regulating the microRNA-466g/SMAD4 signaling pathway. Mol Med Rep 25: 33, 2022.
24. Wang R, Liu Y and Jing L: MiRNA-99a alleviates inflammation and oxidative stress in lipopolysaccharide-stimulated PC-12 cells and rats post spinal cord injury. Bioengineered 13: 4248-4259, 2022.
25. Guo K, Chang Y, Jin Y, Yuan H and Che P: circ-Ncam2 (mmu_circ_0006413) Participates in LPS-Induced Microglia Activation and Neuronal Apoptosis via the TLR4/NF-κB Pathway. J Mol Neurosci 72: 1738-1748, 2022.
26. He X, Zhang J, Guo Y, Yang X, Huang Y and Hao D: Exosomal miR-9-5p derived from BMSCs alleviates apoptosis, inflammation and endoplasmic reticulum stress in spinal cord injury by regulating the HDAC5/FGF2 axis. Mol Immunol 145: 97-108, 2022.
27. Wiatrak B, Kubis-Kubiak A, Piwowar A and Barg E: PC12 cell line: Cell types, coating of culture vessels, differentiation and other culture conditions. Cells 9: 958, 2020.
28. Livak KJ and Schmittgen TD: Analysis of relative gene expression data using real-time quantitative PCR and the 2(-Delta Delta C(T)) method. Methods 25: 402-408, 2001.
29. Li R, Ng TSC, Wang SJ, Prytyskach M, Rodell CB, Mikula H, Kohler RH, Garlin MA, Lauffenburger DA, Parangi S, *et al*: Therapeutically reprogrammed nutrient signalling enhances nanoparticulate albumin bound drug uptake and efficacy in KRAS-mutant cancer. Nat Nanotechnol 16: 830-839, 2021.
30. Zhou J, Li Z, Zhao Q, Wu T, Zhao Q and Cao Y: Knockdown of SNHG1 alleviates autophagy and apoptosis by regulating miR-362-3p/Jak2/stat3 pathway in LPS-injured PC12 cells. Neurochemical Res 46: 945-956, 2021.
31. Huang Y, Li S, Chen H, Feng L, Yuan W and Han T: Butorphanol reduces the neuronal inflammatory response and apoptosis via inhibition of p38/JNK/ATF2/p53 signaling. Exp Ther Med 23: 229, 2022.
32. Ma Z, Lu Y, Yang F, Li S, He X, Gao Y, Zhang G, Ren E, Wang Y and Kang X: Rosmarinic acid exerts a neuroprotective effect on spinal cord injury by suppressing oxidative stress and inflammation via modulating the Nrf2/HO-1 and TLR4/NF-κB pathways. Toxicol Appl Pharmacol 397: 115014, 2020.
33. Samatar AA and Poulikakos PI: Targeting RAS-ERK signalling in cancer: Promises and challenges. Nat Rev Drug Dis 13: 928-942, 2014.
34. Zhang X, Shen R, Shu Z, Zhang Q and Chen Z: S100A12 promotes inflammation and apoptosis in ischemia/reperfusion injury via ERK signaling in vitro study using PC12 cells. Pathol International 70: 403-412, 2020.

35. Yoo SR, Kim Y, Lee MY, Kim OS, Seo CS, Shin HK and Jeong SJ: Gyeji-tang water extract exerts anti-inflammatory activity through inhibition of ERK and NF-κB pathways in lipopolysaccharide-stimulated RAW 264.7 cells. BMC Complement Altern Med 16: 390, 2016.
36. Biswas SK: Does the interdependence between oxidative stress and inflammation explain the antioxidant paradox? Oxid Med Cell Longev 2016: 5698931, 2016.
37. Ganner A, Pfeiffer ZC, Wingendorf L, Kreis S, Klein M, Walz G and Neumann-Haefelin E: The acetyltransferase p300 regulates Nrf2 stability and localization. Biochem Biophys Res Commun 524: 895-902, 2020.
38. Shi Z, Yuan S, Shi L, Li J, Ning G, Kong X and Feng S: Programmed cell death in spinal cord injury pathogenesis and therapy. Cell Prolif 54: e12992, 2021.
39. Zipser CM, Cragg JJ, Guest JD, Fehlings MG, Jutzeler CR, Anderson AJ and Curt A: Cell-based and stem-cell-based treatments for spinal cord injury: Evidence from clinical trials. Lancet Neurol 21: 659-670, 2022.
40. Cunningham CJ, Viskontas M, Janowicz K, Sani Y, Håkansson ME, Heidari A, Huang W and Bo X: The potential of gene therapies for spinal cord injury repair: A systematic review and meta-analysis of pre-clinical studies. Neural Regen Res 18: 299-305, 2023.
41. Chaudhari LR, Kawale AA, Desai SS, Kashte SB and Joshi MG: Pathophysiology of spinal cord injury and tissue engineering approach for its neuronal regeneration: Current status and future prospects. Adv Exp Med Bio: Aug 30, 2022 (Epub ahead of print) doi: 10.1007/5584_2022_731.
42. Karsy M and Hawryluk G: Modern medical management of spinal cord injury. Curr Neurol Neurosci Rep 19: 65, 2019.
43. Anjum A, Yazid MD, Fauzi Daud M, Idris J, Ng AMH, Selvi Naicker A, Ismail OHR, Athi Kumar RK and Lokanathan Y: Spinal cord injury: Pathophysiology, multimolecular interactions, and underlying recovery mechanisms. Int J Mol Sci 21: 7533, 2020.
44. Li X, Zhan J, Hou Y, Hou Y, Chen S, Luo D, Luan J, Wang L and Lin D: Coenzyme Q10 regulation of apoptosis and oxidative stress in H_2O_2 induced BMSC death by modulating the Nrf-2/NQO-1 signaling pathway and its application in a model of spinal cord injury. Oxid Med Cell Longev 2019: 6493081, 2019.
45. Chen S, Ye J, Chen X, Shi J, Wu W, Lin W, Lin W, Li Y, Fu H and Li S: Valproic acid attenuates traumatic spinal cord injury-induced inflammation via STAT1 and NF-κB pathway dependent of HDAC3. J Neuroinflammation 15: 150, 2018.
46. Shen K, Sun G, Chan L, He L, Li X, Yang S, Wang B, Zhang H, Huang J, Chang M, *et al*: Anti-inflammatory nanotherapeutics by targeting matrix metalloproteinases for immunotherapy of spinal cord injury. Small 17: e2102102, 2021.
47. Rodríguez-Cal Y Mayor A, Castañeda-Hernández G, Favari L, Martinez-Cruz A, Guízar-Sahagún G and Cruz-Antonio L: Pharmacokinetics and anti-inflammatory effect of naproxen in rats with acute and subacute spinal cord injury. Naunyn Schmiedebergs Arch Pharmacol 393: 395-404, 2020.
48. Sun B and Kekenes-Huskey PM: Molecular basis of S100A1 activation and target regulation within physiological cytosolic Ca(2+) levels. Front Mol Biosci 7: 77, 2020.
49. Alanazi AM, Fadda L, Alhusaini A, Ahmad R, Hasan IH and Mahmoud AM: Liposomal resveratrol and/or carvedilol attenuate doxorubicin-induced cardiotoxicity by modulating inflammation, oxidative stress and S100A1 in Rats. Antioxidants (Basel) 9: 159, 2020.
50. Zeng Z, Huang N, Zhang Y, Wang Y, Su Y, Zhang H and An Y: CTCF inhibits endoplasmic reticulum stress and apoptosis in cardiomyocytes by upregulating RYR2 via inhibiting S100A1. Life Sci 242: 117158, 2020.
51. Sahu R, Upadhayay S and Mehan S: Inhibition of extracellular regulated kinase (ERK)-1/2 signaling pathway in the prevention of ALS: Target inhibitors and influences on neurological dysfunctions. Eur J Cell Biol 100: 151179, 2021.
52. Ge X, Tang P, Rong Y, Jiang D, Lu X, Ji C, Wang J, Huang C, Duan A, Liu Y, *et al*: Exosomal miR-155 from M1-polarized macrophages promotes EndoMT and impairs mitochondrial function via activating NF-κB signaling pathway in vascular endothelial cells after traumatic spinal cord injury. Redox Biol 41: 101932, 2021.
53. Cheng RD, Ren W, Sun P, Tian L, Zhang L, Zhang J, Li JB and Ye XM: Spinal cord injury causes insulin resistance associated with PI3K signaling pathway in hypothalamus. Neurochem Int 140: 104839, 2020.
54. Xiang Z, Zhang S, Yao X, Xu L, Hu J, Yin C, Chen J and Xu H: Resveratrol promotes axonal regeneration after spinal cord injury through activating Wnt/β-catenin signaling pathway. Aging 13: 23603-23619, 2021.
55. Ciesielska A, Matyjek M and Kwiatkowska K: TLR4 and CD14 trafficking and its influence on LPS-induced pro-inflammatory signaling. Cell Mol Life Sci 78: 1233-1261, 2021.
56. Chen J, Wang Z, Zheng Z, Chen Y, Khor S, Shi K, He Z, Wang Q, Zhao Y, Zhang H, *et al*: Neuron and microglia/macrophage-derived FGF10 activate neuronal FGFR2/PI3K/Akt signaling and inhibit microglia/macrophages TLR4/NF-κB-dependent neuroinflammation to improve functional recovery after spinal cord injury. Cell Death Dis 8: e3090, 2017.